A&A 628, A7 (2019)
https://doi.org/10.1051/0004-6361/201935027

Astronomy & Astrophysics

A meta-analysis of core-collapse supernova ^{56}Ni masses

J. P. Anderson

European Southern Observatory, Alonso de Córdova 3107, Casilla 19, Santiago, Chile
e-mail: janderso@eso.org

Received 7 January 2019 / Accepted 3 June 2019

ABSTRACT

Context. A fundamental property determining the transient behaviour of core-collapse supernovae (CC SNe) is the amount of radioactive ^{56}Ni synthesised in the explosion. Using established methods, this is a relatively easy parameter to extract from observations.
Aims. I provide a meta-analysis of all published ^{56}Ni masses for CC SNe.
Methods. Collating a total of 258 literature ^{56}Ni masses, I compared distributions of the main CC SN types: SNe II, SNe IIb, SNe Ib, SNe Ic, and SNe IcBL.
Results. Using these published values, I calculated a median ^{56}Ni mass of 0.032 $M_{\odot}$ for SNe II (N = 115), 0.102 $M_{\odot}$ for SNe IIb (N = 27), 0.163 $M_{\odot}$ for SNe Ib (N = 33), 0.155 $M_{\odot}$ for SNe Ic (N = 48), and 0.369 $M_{\odot}$ for SNe IcBL (N = 32). On average, stripped-enevelope SNe (SE-SNe: IIb, Ib, Ic, and Ic-BL) have much higher values than SNe II. These observed distributions are compared to those predicted from neutrino-driven explosion models. While the SN II distribution follows model predictions, the SE-SNe have a significant fraction of events with ^{56}Ni masses much higher than predicted.
Conclusions. If the majority of published ^{56}Ni masses are to be believed, these results imply significant differences in the progenitor structures and/or explosion properties between SNe II and SE-SNe. However, such distinct progenitor and explosion properties are not currently favoured in the literature. Alternatively, the popular methods used to estimate ^{56}Ni masses for SE-SNe may not be accurate. Possible issues with these methods are discussed, as are the implications of true ^{56}Ni mass differences on progenitor properties of different CC SNe.

Key words. supernovae: general – stars: massive

1. Introduction

Core-collapse supernovae (CC SNe) are the explosive end of massive stars. A range of physical processes power their electromagnetic output; however, the vast majority of explosions show a common property: they produce a significant amount of radioactive material that powers their luminosity at some epoch. The dominant radioactive decay chain for the first several hundred days of SN evolution is ^{56}Ni to ^{56}Co to ^{56}Fe (Arnett 1996). Therefore, it is of critical importance to know the mass of ^{56}Ni synthesised in the explosion. The amount of ^{56}Ni produced in an explosion is dependent on the explosion properties and the progenitor core structure (see e.g. Ugliano et al. 2012; Pejcha & Thompson 2015; Sukhbold et al. 2016; Suwa et al. 2019 and references therein). How the decay of this material affects the subsequent transient properties then depends on the ejecta structure, the degree to which the ^{56}Ni is mixed outwards, and how asymmetric the ^{56}Ni production is. Constraining the ^{56}Ni yield in different SN types and its effect on their transient behaviour is key to furthering our understanding of massive star explosions.

CC SNe can be broadly separated into two classes: those showing strong, long-lasting hydrogen in their spectra, hydrogen-rich SNe II, and those that do not, hydrogen-poor stripped envelope SNe (SE-SNe). SNe II show a large diversity in their photometric and spectroscopic behaviour (e.g. Anderson et al. 2014; Gutiérrez et al. 2017). However for the purpose of this work SNe II are not split into slower or faster decliners (IIP and IIL, respectively, in historical classification terminology; Barbon et al. 1979) nor peculiar events. Importantly, the vast majority of SNe II are understood to be the result of massive stars exploding with large hydrogen-rich envelopes still present, where their luminosity is powered by shock energy for the first few months post-explosion. Once their initially ionised hydrogen-dominated ejecta are fully recombined, their light curves show a drop in luminosity until they fall onto their radioactively powered s_3 decline (e.g. Anderson et al. 2014).

SE-SNe can be split into different types depending on the presence or absence of specific lines in their optical spectra (see Filippenko 1997 and Gal-Yam 2017 for reviews on SN classification). These differences are thought to imply a sequence of increasing envelope stripping prior to explosion. SNe IIb display hydrogen features in their early-time spectra; however, these features disappear post-maximum light and the SNe transition, and they become more similar to SNe Ib. This latter class lacks hydrogen, but shows strong helium features. Finally, in the spectra of SNe Ic hydrogen and helium are usually both absent (Modjaz et al. 2016)[1]. A small subset of SNe Ic show much broader spectral features and are thus named SNe IcBL (broad line). While SE-SNe display diversity in their light curve properties (absolute magnitudes, decline rates), their overall morphologies are more homogeneous than SNe II, and generally display a characteristic bell-shaped luminosity evolution (see samples of light curves in e.g. Drout et al. 2011; Taddia et al. 2015; Lyman et al. 2016; Prentice et al. 2016; Stritzinger et al. 2018). SE-SNe are therefore understood to be powered by radioactive decay (Arnett 1982) for the vast majority of their evolution (the exception being the very early phases) with the

[1] Although see the case of SN 2016coi (Yamanaka et al. 2017; Prentice et al. 2018).

decay of ^{56}Ni powering the peak luminosity and ^{56}Co becoming dominant several weeks later.

The clear observational differences between SNe II and SE-SNe imply significant differences in progenitor evolution to produce different pre-SN stars that then lead to distinct observational classifications. Initially it was thought that SE-SNe were the result of single Wolf-Rayet (WR) stars (more massive than 25–30 $M_{\odot}$) whose envelopes have been lost through strong stellar winds (e.g. Begelman & Sarazin 1986; Schaeffer et al. 1987). However, there is now mounting evidence (see e.g. Smith 2014 and discussion below) that a significant fraction SE-SNe arise from lower mass progenitors where the envelope stripping is achieved through interaction with a close binary companion (e.g. Podsiadlowski et al. 1992). In this latter scenario SE-SN progenitors have similar initial masses to those of SNe II. Therefore, while the outer structures of progenitors at explosion epoch are different, their inner core structures should be similar. In the single massive star scenario SE-SN and SN II progenitor cores evolve differently due to their distinct initial masses. Given that it is this core structure that determines the resulting details of explosion, constraining how these are similar or different between SN types is important for our understanding of CC SNe.

In the case of SNe II, direct detections of progenitor stars on pre-explosion images has provided strong evidence that the majority arise from red supergiants with initial masses between 8 and 18 $M_{\odot}$ (see Smartt 2015 and references therein). There is some suggestion of a lack of higher mass progenitors, an observation dubbed the "red supergiant problem" (Smartt et al. 2009, although see e.g. Davies & Beasor 2018). Searches for progenitors of SE-SNe have been less conclusive. Eldridge et al. (2013) used 12 non-detections at the explosion sites of SE-SNe to argue against $\geq$25 $M_{\odot}$ Wolf–Rayet stars being their progenitors. However, others have claimed that such progenitors would be hard to detect in the usual band-passes available, given their hot temperatures and correspondingly blue spectral energy distributions (e.g. Yoon et al. 2012).

In recent years, a larger number of possible SE-SN progenitor detections have been published. Van Dyk et al. (2018) and Kilpatrick et al. (2018) have studied the first possible identification of a SN Ic progenitor (SN 2017ein). Both conclude that the visible point source was consistent with a $\geq$45 $M_{\odot}$ initial mass progenitor; however, later observations are required to determine whether the point source is the actual progenitor or a compact cluster[2]. In the case of SNe Ib there is also only one possible progenitor identification, that of iPTF13bvn. While Cao et al. (2013) initially argued for a massive, compact WR star progenitor, Eldridge et al. (2015) and Kim et al. (2015) later revised the pre-explosion photometry and concluded that the progenitor was more likely to be of lower mass (i.e. $\leq$20 $M_{\odot}$, also see Folatelli et al. 2016). The SN IIb class has a larger sample of progenitor detections. All such observations favour low-mass ($\leq$20 $M_{\odot}$) progenitors formed through binary interaction (SN 1993J; e.g. Maund & Smartt 2009, SN 2011dh; e.g. Van Dyk et al. 2013, SN 2016gkg; e.g. Tartaglia et al. 2018). In conclusion, while the statistics are still low, the direct detection of progenitor stars on pre-SN images does not currently favour a significant difference in initial progenitor mass between SNe II anad SE-SNe (although the only possible detection of a SN Ic progenitor is intriguing).

Constraints on pre-SN stars, which are then used to infer zero age main sequence (ZAMS) masses, can also be obtained through modelling SN light curves and spectral velocities. For SNe II, most published results fall within a similar mass range to those of progenitor detections[3] (see e.g. Barbarino et al. 2015), while in some cases hydrodynamic modelling studies have claimed $\geq$20 $M_{\odot}$ progenitors (e.g. Utrobin & Chugai 2017); however, we note the difficulty in inferring initial progenitor mass estimates from hydrogen envelope mass/ejecta constraints (see Dessart & Hillier 2019). SE-SN ejecta masses have been estimated using the application of both analytical and hydrodynamic modelling, with results consistently arguing for low-mass ejecta and therefore low initial progenitor masses consistent with binary evolution and inconsistent with most single-star evolution models (see Drout et al. 2011; Taddia et al. 2015; Lyman et al. 2016; Taddia et al. 2019; Bersten et al. 2018; Prentice et al. 2019). However, there are suggestions that the light curves of some SNe Ic constrain their progenitors to be of higher initial mass (see e.g. Valenti et al. 2012; Taddia et al. 2016).

Less direct constraints on SN progenitors come from analyses of the environments in which they are discovered. Studies of resolved stellar populations surrounding SN explosion sites (Maund 2017, 2018) have argued for a decreasing progenitor age sequence from SNe II through SNe IIb, Ib, and Ic, i.e. an increasing progenitor mass sequence: SNe II-IIb-Ib-Ic. Further afield, studies of unresolved stellar populations have also suggested parent stellar population age differences, with SNe Ic consistently being found within younger stellar populations, and therefore arising from higher mass progenitors than other CC SN types (Anderson et al. 2012; Kangas et al. 2017; Kuncarayakti et al. 2018; Galbany et al. 2018). Finally, SNe IcBL and specifically those accompanying long-duration gamma-ray bursts (GRBs), have environments consistent with coming from the highest mass progenitors of all SNe discussed here (Kelly et al. 2008; Kelly & Kirshner 2012).

In addition to constraints on progenitor ages, environment studies have investigated parent stellar population oxygen abundances, which are then used as progenitor metallicity proxies (Modjaz et al. 2008; Anderson et al. 2010; Leloudas et al. 2011; Sanders et al. 2012b; Kuncarayakti et al. 2018; Galbany et al. 2018; Modjaz et al. 2019). Most CC SN types do not show significant differences, however SNe Ic are consistently found in higher metallicity regions than SNe II and SNe Ib, while SNe IcBL (see Modjaz et al. 2019) are systematically found in galaxies of lower metal abundance than SNe Ic and all other CC SNe. Such metallicity differences may be crucial to explaining the origin of some of the diversity within the CC SN family. These environment studies (both resolved and unresolved) are somewhat in contradiction to the statistical studies of the ejecta masses of SE-SNe discussed above: environment studies suggest significant mass differences between some CC SN types, while estimated ejecta masses suggest very similar initial progenitor masses between SNe II and SE-SNe.

Progenitor mass constraints can also be derived from spectroscopy of SNe at nebular times (several hundred days post-explosion) when the ejecta has become optically thin and the inner core material is revealed. Observations at these epochs constrain the core mass that is predicted to strongly correlate with the ZAMS mass (Woosley et al. 2002). Nebular

[2] If the source is a cluster its spectral energy distribution is also consistent with the SN arising from a very massive progenitor (Van Dyk et al. 2018).

[3] A systematic offset to higher masses from hydrodynamic modelling is often discussed in the literature (see e.g. Bersten et al. 2011). While it may exist, in the main the offset is not huge and does not significantly affect the progenitor mass range for the purpose of the discussion here.

spectroscopic studies have generally concluded for SN II progenitor masses similar to those from direct detections (see e.g. Jerkstrand et al. 2015; Valenti et al. 2016, although see Anderson et al. 2018). Nebular-phase observations of SE-SNe are less common, but the statistical analysis of Fang et al. (2019) concluded that SNe Ic appear to show spectra consistent with more massive progenitors than SNe Ib.

SNe IcBL and those associated with GRBs (in particular) show specific properties that may differentiate them from other CC SNe. Specifically, as mentioned above, the broad-line designation means high ejecta velocities and this implies significantly higher energy explosions than other CC SN types. Significant asphericities have also been discussed to explain the properties of SNe IcBL (Maeda et al. 2003; Dessart et al. 2017). Such high explosion energies are probably inconsistent with these events arising from standard explosion mechanisms (see further discussion below), which brings caveats to discussing their analysis in a similar vain to other types.

In summary, there is a large body of work attempting to constrain CC SN progenitor mass differences. Most studies suggest significant overlap in the ZAMS mass of SNe II and SE-SNe. This suggests that at least a significant fraction of SE-SNe arise through binary evolution (stripping the outer envelope), but from stars with initially very similar masses to SNe II. At the same time, observations do suggest that some SNe Ic arise from more massive progenitors that may evolve as single stars (i.e. they may be massive enough to lose their envelope through stellar winds). Further constraints are required to shed light on progenitor differences between CC SN types and to constrain the explosion mechanism.

As outlined earlier, a critical parameter for understanding how a SN explosion proceeds is the mass of synthesised ^{56}Ni. Müller et al. (2017) compared a sample of observed SN II ^{56}Ni masses with those from explosion models (Sukhbold et al. 2016) finding consistent results. Additional observational samples of SN II ^{56}Ni masses can be found in e.g. Hamuy (2003), Anderson et al. (2014), Spiro et al. (2014), Valenti et al. (2016). SE-SNe are generally analysed separately from SNe II, and various work has provided distributions of ^{56}Ni masses (see e.g. Drout et al. 2011; Lyman et al. 2016; Prentice et al. 2016; Taddia et al. 2015, 2018). This last group of studies present distributions with higher mean ^{56}Ni values than those of SNe II. However, there does not appear to be any formal study analysing SN II and SE-SN ^{56}Ni mass distributions in comparison. This is the aim of the current paper: to provide a meta-analysis of CC SN ^{56}Ni masses to investigate whether there are statistical differences between different CC SN types and to discuss the implications that follow.

This paper is organised as follows. In Sect. 2 I outline how the meta-sample is produced and summairse its characteristics. In Sect. 3 I discuss the main methods used in the literature to estimate ^{56}Ni masses. In Sect. 4 I present ^{56}Ni masses for SN II, SN IIb, SN Ib, SN Ic, and SN IcBL (including GRB-SNe), and compare them statistically. This is followed by a discussion of possible explanations of these results including caveats on the commonly used methods for ^{56}Ni mass estimation in Sect. 5. Final conclusions are presented in Sect. 6.

2. A meta-sample of CC SN ^{56}Ni masses

The aim of this work is to collate and then compare literature CC SN ^{56}Ni masses. In the discussion (Sect. 5) I outline possible systematics in how these values are estimated and how this may affect my results and conclusions. However, here I do not attempt to remeasure ^{56}Ni masses. Following this there is no preference for any specific method for estimating these values. To produce this sample I simply searched the literature for all published masses. Specifically, the SAO/NASA ADS astronomy query form[4] was used, searching for articles with "supernova" and "type II", then "supernova" and "type IIb" and so forth in manuscript abstracts. The resulting lists of articles were then scanned to find published ^{56}Ni masses. While the vast majority of values have probably been collated (through to August 2018)[5], it is probable that some have been missed. In the many cases of multiple literature values for individual SNe a mean mass is calculated. A full reference list for all ^{56}Ni masses can be found in the Appendix. The two main methods for estimating ^{56}Ni in SNe II and SE-SNe are outlined next.

3. Standard procedures to estimate ^{56}Ni masses

While there are many variations on the exact details of how authors estimate ^{56}Ni masses in SNe, there are two standard methods. First, in SNe II the tail luminosity is used as a robust estimate of the synthesised mass of radioactive material. Once the hydrogen ejecta has fully recombined, the light curves of SNe II fall down to their s_3 radioactive tails. At this stage their luminosity is powered by the decay of ^{56}Co. This is clearly established (e.g. Woosley 1988) and the s_3 slope follows the predicted decline (from the rate of decay of ^{56}Co) extremely well in most SNe II (as the radioactive emission is fully trapped by the ejecta; see Anderson et al. 2014 for a discussion of SNe II where this is not the case). It is therefore reasonably straightforward to extract the ^{56}Ni mass using the bolometric luminosity of a SN II if one also has reasonable constraints on the explosion epoch (see e.g. Hamuy 2003 for an outline of one possible procedure).

In the case of SE SNe the tail in the light curves generally decline significantly more quickly than that predicted by the ^{56}Co decay rate (Wheeler et al. 2015) due to incomplete trapping[6]. Therefore, the tail luminosity has not been used for SE-SN ^{56}Ni estimates. SE-SN ^{56}Ni masses are generally estimated using Arnett's rule (Arnett 1982)[7], which states that the SN luminosity at peak brightness equals the instantaneous rate of energy deposition (from radioactive decay). This assumes that radioactive decay is the only energy source at peak magnitude and involves a number of assumptions that are outlined and questioned in Khatami & Kasen (2019) and Dessart et al. (2016) (as will be discussed later). The method used for SE-SNe is therefore more indirect than that for SNe II.

It is important to note the various uncertainties involved in ^{56}Ni mass estimations. The above methods require that observed photometry be converted into bolometric luminosities. Measurements have to be corrected for line-of-sight extinction, distance, and the missing flux outside the observed wavebands. All three of these corrections can have significant uncertainties. In addition, photometry may be contaminated by underlying galaxy light. These observational errors are then summed with those

[4] http://adsabs.harvard.edu/abstract_service.html

[5] Two additional samples were published after this date. Prentice et al. (2019) published a sample of SE SNe, while Taddia et al. (2019) published a sample of SNe IcBL. These additional values are in line with those presented for the meta-sample here, and their inclusion would not affect the results or the conclusions of the present study.

[6] Although 20–30 days post-maxmium most of the emission is trapped and it may be possible to use this epoch in the same way as for SNe II to estimate ^{56}Ni masses (Dessart et al. 2015).

[7] For a fraction of the current meta-sample SE-SN ^{56}Ni masses are estimated through spectral modelling of nebular-phase observations (see e.g. Mazzali et al. 2009), or through modelling of observations around maximum light (see e.g. Bersten et al. 2018).

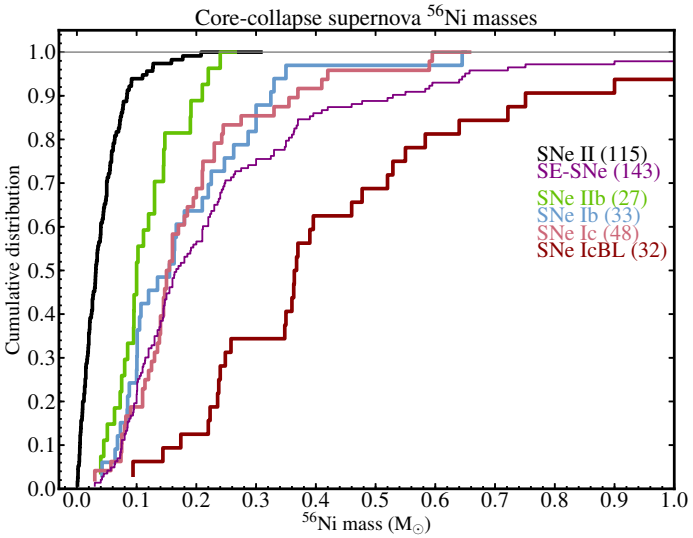

Fig. 1. Cumulative distributions of the ^{56}Ni masses for the different CC SN types analysed in this study. (The SNe IcBL, which includes GRB-SNe, do not complete their cumulative distribution in this figure given that a small number of events are estimated to have synthesised more than 1 $M_\odot$ of ^{56}Ni.)

arising from the ^{56}Ni estimation method. The latter assume an exclusive contribution from ^{56}Ni together with spherical asymmetry. As noted above, Arnett's rule also has a range of assumptions that are not necessarily valid for all SNe.

How these uncertainties may affect the results presented in this work is discussed further in Sect. 5. However, it appears unlikely that they can explain all the differences in ^{56}Ni masses between CC SNe presented here.

4. Results

Figure 1 presents cumulative ^{56}Ni distributions of all CC SNe. Mean, median, and standard deviations for each are presented in Table 1. Table 2 lists the Kolmogorov-Smirnov (KS) statistics between the ^{56}Ni mass distributions of the different types. The SN II distribution is clearly skewed towards significantly lower ^{56}Ni masses than SE-SNe. The median value for the SNe II is a factor of three lower than the SNe IIb and a factor of five lower than the SNe Ib and SNe Ic. The SN II distribution is statistically distinct from all other distributions (Table 2).

Inspecting the minimum and maximum values for each class is also particularly telling: the mininum ^{56}Ni mass for any SE-SN is 0.03 $M_\odot$, while 45% of SNe II have lower values, the lowest being 0.001 $M_\odot$[8]. At the higher end of the SN II distribution there is some overlap with SE-SNe: 100% of the SNe IIb overlap with the SNe II; 76% of the SNe Ib; and 60% of the SNe Ic. In general, it is the lack of low SE-SN ^{56}Ni values that produces such statistically different distributions. The mean value for the ^{56}Ni mass of SN 1987A (the nearest SN to Earth in the last ~400 years) is 0.072 $M_\odot$ and this is often used as the canonical value for SNe II. However, this value is a factor of two higher than the median ^{56}Ni mass of SNe II in the current sample. Indeed, 83% of the SNe II have estimated values lower than SN 1987A. All six events classified as "87A-like" have relatively high ^{56}Ni estimates, with a mean value of 0.086 $M_\odot$.

With respect to differences between the SE-SN classes, the SNe IIb appear to produce less ^{56}Ni than the other types, while there is no statistically significant difference between the SNe Ib and SNe Ic. Meanwhile, the SN IcBL distribution (where GRB-SNe are also included) contains by far the largest number of high masses, with many SNe IcBL estimated to have synthesised more than 0.5 $M_\odot$. To put this in context, Type Ia SNe produce on average 0.6 $M_\odot$ (e.g. Scalzo et al. 2019). As shown in Table 1 and Fig. 1 the SNe Ib and SNe Ic distributions also contain such high values. To see how much these drive the differences seen between SNe II and SE-SNe, the average ^{56}Ni values are recalculated after removing >0.35 $M_\odot$ values. The SNe Ib and SNe Ic mean ^{56}Ni are still a factor of four larger than the SNe II.

The most commonly studied and favoured explosion mechanism for CC SNe is known as the neutrino-driven explosion (see e.g. Janka 2017 for a recent review). Core-collapse is initiated when the iron core becomes too massive to support itself (through degeneracy pressure) against gravity. When the material from this resulting collapse reaches nuclear densities, the collapse is halted and a shock wave drives through the still inwardly falling outer layers of the core. It has long been accepted that the initial shock from the core bounce stagnates. In the neutrino driven mechanism, the huge neutrino flux from the accreting proto-neutron star, assisted by turbulent motions, revives the shock and produces the CC SNe we observe. However, while some simulations have succeeded in producing successful explosions (e.g. Müller et al. 2012), many have not (see discussion in e.g. Takiwaki et al. 2014), and even those that do produce low-energy events. For these reasons, others have proposed alternative explosion mechanisms (see e.g. Papish et al. 2015). A full exploration of alternative models in the context of ^{56}Ni production is beyond the scope of this paper, but the reader should be aware that the comparisons below are made with only a specific theoretical framework that may not be the dominant one in Nature.

A number of studies have provided ^{56}Ni yields from neutrino-driven explosion models of various levels of complexity (Ugliano et al. 2012; Pejcha & Thompson 2015; Sukhbold et al. 2016; Suwa et al. 2019[9], ^{56}Ni yields from other models are discussed below). While the exact results vary between studies (e.g. the dependence of the synthesised ^{56}Ni on explosion energy and initial progenitor mass), the predicted ^{56}Ni mass range is somewhat similar, as is the maximum predicted value. In the case of SNe II, Müller et al. (2017) showed that the ^{56}Ni distribution predicted by Sukhbold et al. (2016) was in reasonable agreement with observed SNe II, and qualitatively we find the same result here with a much larger sample. SE-SNe however, have estimated values in significant excess of model predictions. The maximum predicted value in each of the four explosion model studies cited above is 0.15 $M_\odot$ (Ugliano et al. 2012); 0.2 $M_\odot$ (Pejcha & Thompson 2015); 0.171 $M_\odot$ (Sukhbold et al. 2016); and 0.226 $M_\odot$ (Suwa et al. 2019). Taking the most extreme of these (0.226 $M_\odot$), 30% of SN Ib have higher inferred values, together with 29% of SNe Ic and 84% of SNe IcBL (only 3%

[8] This may suggest an observational bias against detecting SE-SNe with low ^{56}Ni masses. Such SNe would be much dimmer than the observed SE-SN population and may have gone undetected. If this is the case, then we should expect the current and future generation of discovery surveys, which search deeper and with a higher cadence than ever before, to start detecting such events.

[9] Most of these works only model the initial explosion and the estimated nucleosynthesis; they do not go on to produce light curves or spectra that can be compared to observed events. Sukhbold et al. (2016) produce such observables, and their explosions struggle to reproduce the observed SE-SNe.

Table 1. CC SN ^{56}Ni statistics.

SN distribution (N)	Mean ($M_\odot$)	Standard deviation ($M_\odot$)	Median ($M_\odot$)	Max ($M_\odot$)	Min ($M_\odot$)
SN II (115)	0.044	0.044	0.032	0.360	0.001
SE-SN (143)	0.293	0.295	0.184	2.400	0.030
SN IIb (27)	0.124	0.061	0.102	0.280	0.030
SN Ib (33)	0.199	0.146	0.163	0.920	0.030
SN Ic (48)	0.198	0.139	0.155	0.840	0.030
SN IcBL (32)	0.507	0.410	0.369	2.400	0.070

Notes. In Col. 1 are listed the SN distribution and the number of events within that distribution in brackets. Means, standard deviations, and medians of the distributions are then presented in Cols. 2–4, respectively. In the last two columns are listed the minimum and maximum value in each distribution (from the individual literature measurements, while in Fig. 1 the mean values for each SN are plotted).

Table 2. KS statistical differences between the various different CC SN ^{56}Ni distributions.

SN distributions (N)	D	p
SN II (115)–SE-SNe (143)	0.773	1.2×10^{-34}
SN II (115)–SN IIb (27)	0.687	6.1×10^{-10}
SN II (115)–SN Ib (33)	0.774	1.5×10^{-14}
SN II (115)–SN Ic (48)	0.801	3.0×10^{-20}
SN IIb (27)–SN Ib (33)	0.323	0.07
SN IIb (27)–SN Ic (48)	0.375	0.01
SN Ib (33)–SN Ic (48)	0.227	0.23
SN Ic (48)–SN IcBL (32)	0.635	1.3×10^{-7}

Notes. In Col. 1 the two distributions being compared are listed together with the number of events within each distribution in brackets. In Col. 2 the D parameter is given, while in the last column the p value is presented.

of SN II and 7% of SNe IIb have values in excess of this limit). Therefore, even in the most optimistic case (that many of the SE-SNe come from the highest values from explosion model predictions), a significant fraction of ^{56}Ni estimated values for SE-SNe are outside of neutrino-driven model estimations[10]. As Fig. 1 shows, a number of SE-SNe have values twice or even three times as large as this limit. The implications of these results, together with a series of caveats and possible explanations, are now discussed.

5. Discussion

Two main results are presented in this paper: first, that values of ^{56}Ni in the literature are systematically larger for SE-SNe than for SNe II and second, that a significant fraction of SE-SNe have published ^{56}Ni masses in excess of the largest masses predicted by a range of different neutrino-driven explosion models. The first result implies significant differences in the progenitor structures and explosion properties between hydrogen-rich and hydrogen-poor CC SNe. However, the second result may suggest that the estimates for many SE-SNe are significantly in error or that the currently most popular explosion model (neutrino-driven explosion) is not applicable to a significant fraction of CC SNe.

The general current consensus (although it is still debated) is that a significant fraction of SE-SNe, if not the vast majority, arise from binary systems where mass transfer is responsible for removing the outer hydrogen-rich (types IIb, Ib) and helium-rich (Ic) layers of the progenitors. In this hypothesis, the initial progenitor masses of SNe II and SE-SNe are similar (although those of SE-SNe are still probably higher on average). While their pre-SN outer structures are distinct, their core structures should be somewhat indistinguishable (in most cases the core will evolve independently of surface processes). Therefore, it is not clear how it is possible to arrive at such distinct ^{56}Ni masses (as presented in this study) if the progenitors have similar initial masses. If we postulate that SE-SNe actually have significantly more massive progenitors (and evolve either as single stars or in binary systems) then we can speculate that their cores have more material at sufficiently high densities to produce higher amounts of ^{56}Ni during the explosion. However, this is not actually predicted by neutrino-driven explosion models (Ugliano et al. 2012; Pejcha & Thompson 2015; Sukhbold et al. 2016; Suwa et al. 2019): a 25 $M_\odot$ star does not necessarily produce more ^{56}Ni than an 15 $M_\odot$ star, for example, and models do not produce ^{56}Ni masses in excess of 0.2 $M_\odot$. In summary, if literature ^{56}Ni values are to be believed, then (a) the progenitor structures (and by inference the initial progenitor properties) must be significantly more different between SNe II and SE-SNe than currently believed, and (b) progenitor structures and/or explosion properties of SE-SNe must be distinct from those predicted by stellar evolution and currently favoured explosion models.

There are various sources of observational error that may affect ^{56}Ni mass estimates: (1) errors in photometry; (2) errors in SN distances; (3) errors in extinction corrections; and (4) errors in bolometric corrections. If any of these corrections are systematically wrong for one SN type compared to another, this may produce some of the differences that we observe. The errors from group 1 can be assumed to be negligible compared to the rest. There is no reason to believe that errors in distances are any different between SN types (although very large or very small individual ^{56}Ni masses may be due to distance errors).

The estimation of accurate host galaxy extinctions for CC SNe is notoriously difficult (see recent discussion for the case of SNe II: de Jaeger et al. 2018). These estimates are generally derived by assuming some uniform intrinsic colour for a given SN type and correcting assumed reddened SNe to assumed unreddened events (see e.g. Stritzinger et al. 2018), or by measuring the strength of absorption from interstellar sodium (see e.g. Phillips et al. 2013). However, both of these methods have strong caveats. To investigate how these errors may affect the results from the current study, I also compiled host galaxy extinction estimates employed by each study contributing ^{56}Ni masses to this work. The median host galaxy visual extinction does increase from hydrogen-rich through the stripped-envelope classes (0.12 mag for SNe II; 0.25 mag for SNe IIb; 0.30 mag for

[10] Although see Umeda & Nomoto (2008) for much higher ^{56}Ni masses produced from SNe more massive than 30 $M_\odot$.

SNe Ib; and 0.56 mag for SNe Ic), while for the SNe IcBL the median is 0.12 mag. However, this is somewhat expected, given the increasing sequence of association from SNe II through to SNe Ic to bright H II regions (Anderson et al. 2012, where higher levels of extinction are expected). Still, in the extreme case of assuming that the host extinction estimates are systematically wrong, for example between SNe II and SNe Ic, we can estimate that the addition of 0.44 visual magnitudes (the difference in the median values of SNe II and SNe Ic) to the bolometric luminosity of a SN II would only increase the median ^{56}Ni value to 0.048 $M_{\odot}$. In order to increase this to the median of the SNe Ic (0.155 $M_{\odot}$), a difference of 1.7 mag is required. It seems extremely unlikely that such a difference has gone unnoticed.

Finally, if there were a systematic error in the way bolometric corrections were applied between SNe II and SE-SNe this could produce some difference in ^{56}Ni masses. Bolometric corrections are either produced by using very well observed (in wavelength) SNe as templates and assuming similar spectral energy distributions for less well-observed events, or through comparison to models. In this study ^{56}Ni masses are compiled from many different sources and in many SNe there are multiple values (up to eight) from different studies. Comparing these values can give some idea of the differences resulting from different bolometric corrections. In the case of SNe II the mean standard deviation of multiple ^{56}Ni mass estimates is 0.013 $M_{\odot}$, while for SNe Ic it is 0.06 $M_{\odot}$. If we assume that this larger scatter for the SNe Ic is due to systematically incorrect bolometric corrections for some of the estimates for these SNe, then we can speculate that such an error propagates to differences in ^{56}Ni mass estimates. However, the above difference is not sufficient to explain the significantly distinct ^{56}Ni distributions. In summary, there does not appear to be any significantly large observational error that would negate the conclusion of large differences between the estimated ^{56}Ni masses of SNe II and SE-SNe.

The methodology for estimating ^{56}Ni masses from SN II observations is understood to be robust in a theoretical sense. However, doubt has often been cast as to the accuracy of using Arnett's rule in the case of SE-SNe (the methodology used for the vast majority of literature values compiled here). Katz et al. (2013) published an "exact integral relation between the ^{56}Ni mass and the bolometric light curve", arguing that this overcomes issues with Arnett's rule such as assumed opacities, density distribution, and the ^{56}Ni deposition distribution into the ejecta. Dessart et al. (2015, 2016) published radiative transfer models of SE-SNe (IIb/Ib/Ic) based on explosions of the mass donor in a close-binary system. These authors concluded that for this set of models Arnett's rule overestimates the ^{56}Ni mass by around 50% (while suggesting that the Katz et al. 2013 procedure yields more reliable values). However, these models (and explosion models of SE-SNe in general, see e.g. Sukhbold et al. 2016 for another example) often struggle to accurately reproduce observations; for example, the model rise times are longer than those observed. More recently, Khatami & Kasen (2019) discussed in detail the assumptions that are contained within the classical Arnett model and argued, using comparison to numerical simulations, that Arnett's rule does not hold in general (while presenting new analytic relations), and is only valid in certain explosion configurations. It is important to note that the published values between SNe II and SNe Ib/SNe Ic differ by a factor of five (Sect. 4). This is significantly larger than the offsets discussed in Dessart et al. (2015) and Khatami & Kasen (2019), among others.

As discussed above, the neutrino-driven explosion mechanism may not be at play in all CC SNe. Soker (2018) argues that jets are required to explode many if not all CC SNe, and that a paradigm shift is needed to move away from the neutrino-driven mechanism to a "jet-driven explosion mechanism that is aided by neutrino heating". However, there are few studies of nucleosynthetic yields from non-standard explosion models (to my knowledge). Barnes et al. (2018) presented a model of a GRB central engine producing the accompanying SN IcBL through a jet-driven aspherical explosion. Aspherical explosions may be applicable to the majority of SE-SNe, given the number of such events showing double-peaked nebular-phase spectral features (Maeda et al. 2008). This model calculated the synthesised ^{56}Ni mass through a temperature condition, and estimated a yield of 0.24 $M_{\odot}$ of ^{56}Ni. This is higher than for any of the explosion models discussed above, but it should be noted that there are many SE-SNe (and not just the IcBLs) in Fig. 1 that have values in excess of this. Additional explosion and nucleosyhthesis modelling is required to understand whether alternative models can indeed consistently produce ^{56}Ni masses much higher than 0.2 $M_{\odot}$.

In the case of SNe IcBL estimated ^{56}Ni masses are extremely large, being of the same order as those for SNe Ia, together with a tail out to values higher than 1 $M_{\odot}$. This seems to be beyond any available progenitor exploded through the neutrino-driven explosion model. As noted previously, one possibility is that SN IcBL explosions are significantly asymmetric, and we observe these events as SNe IcBL when the explosion direction is towards the observer (see e.g. Maeda et al. 2003; Dessart et al. 2017). In such cases ^{56}Ni masses derived assuming spherical symmetry (e.g. Arnett's rule) will be overestimated (Dessart et al. 2017, and ejecta masses will be underestimated). This explanation cannot work for the SE-SN sample at large as statistically one would expect to observe both high and low values depending on the viewing angle of the observer.

Finally, a remaining explanation is simply that for many SE-SNe radioactive decay is not the dominant power source of their luminosity. If an additional power source is present (e.g. a magnetar) then assuming that all the power comes exclusively from ^{56}Ni will lead to an overestimate of these masses.

6. Conclusions

Using published ^{56}Ni masses from the literature that employ standard methods for estimating the contribution of radioactive decay power to SN luminosities, I have shown that hydrogen-poor SE-SNe are estimated to produce around five times more ^{56}Ni than hydrogen-rich SNe II. This difference is highly statistically significant. While the distribution of ^{56}Ni for SNe II agrees with predictions from neutrino-driven explosion models, that of SE-SNe does not. These results imply that either SE-SN progenitors and their subsequent explosions are significantly distinct from those of SNe II, or that there is a systematic error in how ^{56}Ni masses are calculated. This work serves to highlight these issues to the community. The amount of radioactive material synthesised in CC SNe is a critical parameter in understanding these explosive events. Therefore, a detailed understanding of how well we derive this property is vital in order to move our understanding forward.

Acknowledgements. The anonymous referee is thanked for the comments and suggestions. Luc Dessart is thanked for providing detailed comments on a draft version of this manuscript. In addition, I acknowledge fruitful conversations with the following people that aided in the discussion sections of this paper: Takashi Moriya, Ondřej Pejcha, Tomas Müller, José Luis Prieto, Keiichi Maeda, Melina Bersten, and Peter Hoeflich.

References

Anderson, J. P., Covarrubias, R. A., James, P. A., Hamuy, M., & Habergham, S. M. 2010, MNRAS, 407, 2660
Anderson, J. P., Habergham, S. M., James, P. A., & Hamuy, M. 2012, MNRAS, 424, 1372
Anderson, J. P., González-Gaitán, S., Hamuy, M., et al. 2014, ApJ, 786, 67
Anderson, J. P., Dessart, L., Gutiérrez, C. P., et al. 2018, Nat. Astron., 2, 574
Andrews, J. E., Sugerman, B. E. K., Clayton, G. C., et al. 2011, ApJ, 731, 47
Anupama, G. C., Sahu, D. K., Deng, J., et al. 2005, ApJ, 631, L125
Arnett, D. 1996, Supernovae and Nucleosynthesis: An Investigation of the History of Matter from the Big Bang to the Present (Princeton: Princeton University Press), 559
Arnett, W. D. 1982, ApJ, 253, 785
Arnett, W. D., Bahcall, J. N., Kirshner, R. P., & Woosley, S. E. 1989, ARA&A, 27, 629
Barbarino, C., Dall'Ora, M., Botticella, M. T., et al. 2015, MNRAS, 448, 2312
Barbon, R., Ciatti, F., & Rosino, L. 1979, A&A, 72, 287
Barnes, J., Duffell, P. C., Liu, Y., et al. 2018, ApJ, 860, 38
Begelman, M. C., & Sarazin, C. L. 1986, ApJ, 302, L59
Ben-Ami, S., Gal-Yam, A., Filippenko, A. V., et al. 2012, ApJ, 760, L33
Benetti, S., Turatto, M., Valenti, S., et al. 2011, MNRAS, 411, 2726
Berger, E., Chornock, R., Holmes, T. R., et al. 2011, ApJ, 743, 204
Bersten, M. C., Benvenuto, O., & Hamuy, M. 2011, ApJ, 729, 61
Bersten, M. C., Benvenuto, O. G., Nomoto, K. I., et al. 2012, ApJ, 757, 31
Bersten, M. C., Folatelli, G., García, F., et al. 2018, Nature, 554, 497
Bose, S., Kumar, B., Sutaria, F., et al. 2013, MNRAS, 433, 1871
Bose, S., Sutaria, F., Kumar, B., et al. 2015, ApJ, 806, 160
Bufano, F., Pian, E., Sollerman, J., et al. 2012, ApJ, 753, 67
Bufano, F., Pignata, G., Bersten, M., et al. 2014, MNRAS, 439, 1807
Cano, Z., Izzo, L., de Ugarte Postigo, A., et al. 2017, A&A, 605, A107
Cao, Y., Kasliwal, M. M., Arcavi, I., et al. 2013, ApJ, 775, L7
Chen, J., Wang, X., Ganeshalingam, M., et al. 2014, ApJ, 790, 120
Clocchiatti, A., Phillips, M. M., Suntzeff, N. B., et al. 2000, ApJ, 529, 661
Corsi, A., Ofek, E. O., Frail, D. A., et al. 2011, ApJ, 741, 76
Corsi, A., Cenko, S. B., Kasliwal, M. M., et al. 2017, ApJ, 847, 54
Dastidar, R., Misra, K., Hosseinzadeh, G., et al. 2018, MNRAS, 479, 2421
Davies, B., & Beasor, E. R. 2018, MNRAS, 474, 2116
de Jaeger, T., Anderson, J. P., Galbany, L., et al. 2018, MNRAS, 476, 4592
D'Elia, V., Pian, E., Melandri, A., et al. 2015, A&A, 577, A116
Deng, J., Tominaga, N., Mazzali, P. A., Maeda, K., & Nomoto, K. 2005, ApJ, 624, 898
Dessart, L., & Hillier, D. J. 2019, A&A, 625, A9
Dessart, L., Hillier, D. J., Woosley, S., et al. 2015, MNRAS, 453, 2189
Dessart, L., Hillier, D. J., Woosley, S., et al. 2016, MNRAS, 458, 1618
Dessart, L., John Hillier, D., Yoon, S.-C., Waldman, R., & Livne, E. 2017, A&A, 603, A51
Dhungana, G., Kehoe, R., Vinko, J., et al. 2016, ApJ, 822, 6
Drout, M. R., Soderberg, A. M., Gal-Yam, A., et al. 2011, ApJ, 741, 97
Eldridge, J. J., Fraser, M., Smartt, S. J., Maund, J. R., & Crockett, R. M. 2013, MNRAS, 436, 774
Eldridge, J. J., Fraser, M., Maund, J. R., & Smartt, S. J. 2015, MNRAS, 446, 2689
Elmhamdi, A., Chugai, N. N., & Danziger, I. J. 2003, A&A, 404, 1077
Elmhamdi, A., Tsvetkov, D., Danziger, I. J., & Kordi, A. 2011, ApJ, 731, 129
Fang, Q., Maeda, K., Kuncarayakti, H., Sun, F., & Gal-Yam, A. 2019, Nat. Astron., 3, 434
Filippenko, A. V. 1997, ARA&A, 35, 309
Folatelli, G., Contreras, C., Phillips, M. M., et al. 2006, ApJ, 641, 1039
Folatelli, G., Bersten, M. C., Kuncarayakti, H., et al. 2014, ApJ, 792, 7
Folatelli, G., Van Dyk, S. D., Kuncarayakti, H., et al. 2016, ApJ, 825, L22
Foley, R. J., Papenkova, M. S., Swift, B. J., et al. 2003, PASP, 115, 1220
Fremling, C., Sollerman, J., Taddia, F., et al. 2016, A&A, 593, A68
Gal-Yam, A. 2017, Observational and Physical Classification of Supernovae (Cham: Springer), 195
Galbany, L., Anderson, J. P., Sánchez, S. F., et al. 2018, ApJ, 855, 107
Gangopadhyay, A., Misra, K., Pastorello, A., et al. 2018, MNRAS, 476, 3611
Gurugubelli, U. K., Sahu, D. K., Anupama, G. C., & Chakradhari, N. K. 2008, Bull. Astron. Soc. India, 36, 79
Gutiérrez, C. P., Anderson, J. P., Hamuy, M., et al. 2017, ApJ, 850, 89
Hamuy, M. 2003, ApJ, 582, 905
Hamuy, M., Deng, J., Mazzali, P. A., et al. 2009, ApJ, 703, 1612
Hendry, M. A., Smartt, S. J., Maund, J. R., et al. 2005, MNRAS, 359, 906
Hosseinzadeh, G., Valenti, S., McCully, C., et al. 2018, ApJ, 861, 63
Huang, F., Wang, X., Zhang, J., et al. 2015, ApJ, 807, 59
Huang, F., Wang, X. F., Hosseinzadeh, G., et al. 2018, MNRAS, 475, 3959
Inserra, C., Pastorello, A., Turatto, M., et al. 2013, A&A, 555, A142
Iwamoto, K., Nomoto, K., Höflich, P., et al. 1994, ApJ, 437, L115
Iwamoto, K., Mazzali, P. A., Nomoto, K., et al. 1998, Nature, 395, 672
Janka, H. T. 2017, Neutrino-Driven Explosions (Cham: Springer), 1095
Jerkstrand, A., Smartt, S. J., Sollerman, J., et al. 2015, MNRAS, 448, 2482
Kangas, T., Blagorodnova, N., Mattila, S., et al. 2017, MNRAS, 469, 1246
Katz, B., Kushnir, D., & Dong, S. 2013, ArXiv e-prints [arXiv:1301.6766]
Kelly, P. L., & Kirshner, R. P. 2012, ApJ, 759, 107
Kelly, P. L., Kirshner, R. P., & Pahre, M. 2008, ApJ, 687, 1201
Khatami, D. K., & Kasen, D. N. 2019, ApJ, 878, 56
Kilpatrick, C. D., Takaro, T., Foley, R. J., et al. 2018, MNRAS, 480, 2072
Kim, H.-J., Yoon, S.-C., & Koo, B.-C. 2015, ApJ, 809, 131
Kleiser, I. K. W., Poznanski, D., Kasen, D., et al. 2011, MNRAS, 415, 372
Kumar, B., Pandey, S. B., Sahu, D. K., et al. 2013, MNRAS, 431, 308
Kumar, B., Singh, A., Srivastav, S., Sahu, D. K., & Anupama, G. C. 2018, MNRAS, 473, 3776
Kuncarayakti, H., Anderson, J. P., Galbany, L., et al. 2018, A&A, 613, A35
Leloudas, G., Gallazzi, A., Sollerman, J., et al. 2011, A&A, 530, A95
Lisakov, S. M., Dessart, L., Hillier, D. J., Waldman, R., & Livne, E. 2017, MNRAS, 466, 34
Liu, Z., Zhao, X.-L., Huang, F., et al. 2015, Res. Astron. Astrophys., 15, 225
Lyman, J. D., Bersier, D., James, P. A., et al. 2016, MNRAS, 457, 328
Maeda, K., Mazzali, P. A., Deng, J., et al. 2003, ApJ, 593, 931
Maeda, K., Kawabata, K., Mazzali, P. A., et al. 2008, Science, 319, 1220
Maund, J. R. 2017, MNRAS, 469, 2202
Maund, J. R. 2018, MNRAS, 476, 2629
Maund, J. R., & Smartt, S. J. 2009, Science, 324, 486
Mazzali, P. A., Deng, J., Tominaga, N., et al. 2003, ApJ, 599, L95
Mazzali, P. A., Deng, J., Maeda, K., et al. 2004, ApJ, 614, 858
Mazzali, P. A., Deng, J., Pian, E., et al. 2006, ApJ, 645, 1323
Mazzali, P. A., Valenti, S., Della Valle, M., et al. 2008, Science, 321, 1185
Mazzali, P. A., Deng, J., Hamuy, M., & Nomoto, K. 2009, ApJ, 703, 1624
Mazzali, P. A., Sauer, D. N., Pian, E., et al. 2017, MNRAS, 469, 2498
Melandri, A., Pian, E., Ferrero, P., et al. 2012, A&A, 547, A82
Melandri, A., Pian, E., D'Elia, V., et al. 2014, A&A, 567, A29
Milisavljevic, D., Soderberg, A. M., Margutti, R., et al. 2013a, ApJ, 770, L38
Milisavljevic, D., Margutti, R., Soderberg, A. M., et al. 2013b, ApJ, 767, 71
Milisavljevic, D., Margutti, R., Parrent, J. T., et al. 2015, ApJ, 799, 51
Modjaz, M., Kewley, L., Kirshner, R. P., et al. 2008, AJ, 135, 1136
Modjaz, M., Liu, Y. Q., Bianco, F. B., & Graur, O. 2016, ApJ, 832, 108
Modjaz, M., Bianco, F. B., Siwek, M., et al. 2019, ApJ, submitted [arXiv:1901.00872]
Morales-Garoffolo, A., Elias-Rosa, N., Bersten, M., et al. 2015, MNRAS, 454, 95
Müller, B., Janka, H.-T., & Heger, A. 2012, ApJ, 761, 72
Müller, T., Prieto, J. L., Pejcha, O., & Clocchiatti, A. 2017, ApJ, 841, 127
Nadyozhin, D. K. 2003, MNRAS, 346, 97
Nakamura, T., Mazzali, P. A., Nomoto, K., & Iwamoto, K. 2001, ApJ, 550, 991
Oates, S. R., Bayless, A. J., Stritzinger, M. D., et al. 2012, MNRAS, 424, 1297
Otsuka, M., Meixner, M., Panagia, N., et al. 2012, ApJ, 744, 26
Papish, O., Nordhaus, J., & Soker, N. 2015, MNRAS, 448, 2362
Pastorello, A., Zampieri, L., Turatto, M., et al. 2004, MNRAS, 347, 74
Pastorello, A., Baron, E., Branch, D., et al. 2005, MNRAS, 360, 950
Pastorello, A., Valenti, S., Zampieri, L., et al. 2009, MNRAS, 394, 2266
Pastorello, A., Pumo, M. L., Navasardyan, H., et al. 2012, A&A, 537, A141
Pejcha, O., & Prieto, J. L. 2015, ApJ, 799, 215
Pejcha, O., & Thompson, T. A. 2015, ApJ, 801, 90
Phillips, M. M., Simon, J. D., Morrell, N., et al. 2013, ApJ, 779, 38
Pian, E., Tomasella, L., Cappellaro, E., et al. 2017, MNRAS, 466, 1848
Pignata, G., Stritzinger, M., Soderberg, A., et al. 2011, ApJ, 728, 14
Podsiadlowski, P., Joss, P. C., & Hsu, J. J. L. 1992, ApJ, 391, 246
Prentice, S. J., Mazzali, P. A., Pian, E., et al. 2016, MNRAS, 458, 2973
Prentice, S. J., Ashall, C., Mazzali, P. A., et al. 2018, MNRAS, 478, 4162
Prentice, S. J., Ashall, C., James, P. A., et al. 2019, MNRAS, 485, 1559
Richardson, D., Branch, D., & Baron, E. 2006, AJ, 131, 2233
Roming, P. W. A., Pritchard, T. A., Brown, P. J., et al. 2009, ApJ, 704, L118
Roy, R., Kumar, B., Moskvitin, A. S., et al. 2011a, MNRAS, 414, 167
Roy, R., Kumar, B., Benetti, S., et al. 2011b, ApJ, 736, 76
Roy, R., Kumar, B., Maund, J. R., et al. 2013, MNRAS, 434, 2032
Roy, R., Sollerman, J., Silverman, J. M., et al. 2016, A&A, 596, A67
Sahu, D. K., Tanaka, M., Anupama, G. C., Gurugubelli, U. K., & Nomoto, K. 2009, ApJ, 697, 676
Sahu, D. K., Anupama, G. C., Chakradhari, N. K., et al. 2018, MNRAS, 475, 2591
Sanders, N. E., Soderberg, A. M., Valenti, S., et al. 2012a, ApJ, 756, 184
Sanders, N. E., Soderberg, A. M., Levesque, E. M., et al. 2012b, ApJ, 758, 132
Sauer, D. N., Mazzali, P. A., Deng, J., et al. 2006, MNRAS, 369, 1939
Scalzo, R. A., Parent, E., Burns, C., et al. 2019, MNRAS, 483, 628
Schaeffer, R., Casse, M., & Cahen, S. 1987, ApJ, 316, L31

Shigeyama, T., Suzuki, T., Kumagai, S., et al. 1994, ApJ, 420, 341
Silverman, J. M., Mazzali, P., Chornock, R., et al. 2009, PASP, 121, 689
Smartt, S. J. 2015, PASA, 32, e016
Smartt, S. J., Eldridge, J. J., Crockett, R. M., & Maund, J. R. 2009, MNRAS, 395, 1409
Smith, N. 2014, ARA&A, 52, 487
Soker, N. 2018, Res. Astron. Astrophys., submitted [arXiv:1810.09074]
Spiro, S., Pastorello, A., Pumo, M. L., et al. 2014, MNRAS, 439, 2873
Srivastav, S., Anupama, G. C., & Sahu, D. K. 2014, MNRAS, 445, 1932
Stritzinger, M., Hamuy, M., Suntzeff, N. B., et al. 2002, AJ, 124, 2100
Stritzinger, M., Mazzali, P., Phillips, M. M., et al. 2009, ApJ, 696, 713
Stritzinger, M. D., Taddia, F., Burns, C. R., et al. 2018, A&A, 609, A135
Sukhbold, T., Ertl, T., Woosley, S. E., Brown, J. M., & Janka, H.-T. 2016, ApJ, 821, 38
Suwa, Y., Tominaga, N., & Maeda, K. 2019, MNRAS, 483, 3607
Szalai, T., Vinkó, J., Nagy, A. P., et al. 2016, MNRAS, 460, 1500
Taddia, F., Stritzinger, M. D., Sollerman, J., et al. 2012, A&A, 537, A140
Taddia, F., Sollerman, J., Leloudas, G., et al. 2015, A&A, 574, A60
Taddia, F., Fremling, C., Sollerman, J., et al. 2016, A&A, 592, A89
Taddia, F., Stritzinger, M. D., Bersten, M., et al. 2018, A&A, 609, A136
Taddia, F., Sollerman, J., Fremling, C., et al. 2019, A&A, 621, A71
Takaki, K., Kawabata, K. S., Yamanaka, M., et al. 2013, ApJ, 772, L17
Takáts, K., Pignata, G., Pumo, M. L., et al. 2015, MNRAS, 450, 3137
Takiwaki, T., Kotake, K., & Suwa, Y. 2014, ApJ, 786, 83
Tartaglia, L., Sand, D. J., Valenti, S., et al. 2018, ApJ, 853, 62
Taubenberger, S., Pastorello, A., Mazzali, P. A., et al. 2006, MNRAS, 371, 1459
Taubenberger, S., Navasardyan, H., Maurer, J. I., et al. 2011, MNRAS, 413, 2140
Terreran, G., Jerkstrand, A., Benetti, S., et al. 2016, MNRAS, 462, 137
Tomasella, L., Cappellaro, E., Pumo, M. L., et al. 2018, MNRAS, 475, 1937
Tominaga, N., Limongi, M., Suzuki, T., et al. 2008, ApJ, 687, 1208
Tomita, H., Deng, J., Maeda, K., et al. 2006, ApJ, 644, 400
Tsvetkov, D. Y., Shugarov, S. Y., Volkov, I. M., et al. 2018, Astron. Lett., 44, 315
Turatto, M., Mazzali, P. A., Young, T. R., et al. 1998, ApJ, 498, L129
Ugliano, M., Janka, H.-T., Marek, A., & Arcones, A. 2012, ApJ, 757, 69
Umeda, H., & Nomoto, K. 2008, ApJ, 673, 1014
Utrobin, V. P., & Chugai, N. N. 2017, MNRAS, 472, 5004
Valenti, S., Elias-Rosa, N., Taubenberger, S., et al. 2008, ApJ, 673, L155
Valenti, S., Fraser, M., Benetti, S., et al. 2011, MNRAS, 416, 3138
Valenti, S., Taubenberger, S., Pastorello, A., et al. 2012, ApJ, 749, L28
Valenti, S., Sand, D., Stritzinger, M., et al. 2015, MNRAS, 448, 2608
Valenti, S., Howell, D. A., Stritzinger, M. D., et al. 2016, MNRAS, 459, 3939
Van Dyk, S. D., Zheng, W., Clubb, K. I., et al. 2013, ApJ, 772, L32
Van Dyk, S. D., Zheng, W., Brink, T. G., et al. 2018, ApJ, 860, 90
Vinkó, J., Takáts, K., Sárneczky, K., et al. 2006, MNRAS, 369, 1780
Walker, E. S., Mazzali, P. A., Pian, E., et al. 2014, MNRAS, 442, 2768
Wheeler, J. C., Johnson, V., & Clocchiatti, A. 2015, MNRAS, 450, 1295
Woosley, S. E. 1988, ApJ, 330, 218
Woosley, S. E., Heger, A., & Weaver, T. A. 2002, Rev. Mod. Phys., 74, 1015
Yamanaka, M., Nakaoka, T., Tanaka, M., et al. 2017, ApJ, 837, 1
Yoon, S. C., Gräfener, G., Vink, J. S., Kozyreva, A., & Izzard, R. G. 2012, A&A, 544, L11
Yuan, F., Jerkstrand, A., Valenti, S., et al. 2016, MNRAS, 461, 2003
Zampieri, L., Pastorello, A., Turatto, M., et al. 2003, MNRAS, 338, 711
Zhang, J., Wang, X., Vinkó, J., et al. 2018, ApJ, 863, 109

Appendix A: Reference list for ^{56}Ni mass values

Here all the references used to compile the meta-sample of CC SN ^{56}Ni values used in this work are listed.

SNe II: Arnett et al. (1989), Turatto et al. (1998), Nadyozhin (2003), Hamuy (2003), Elmhamdi et al. (2003), Zampieri et al. (2003), Pastorello et al. (2004, 2005, 2009, 2012), Hendry et al. (2005), Vinkó et al. (2006), Gurugubelli et al. (2008), Kleiser et al. (2011), Bersten et al. (2011), Andrews et al. (2011), Roy et al. (2011a,b), Taddia et al. (2012), Otsuka et al. (2012), Inserra et al. (2013), Bose et al. (2013, 2015), Spiro et al. (2014), Pejcha & Prieto (2015), Huang et al. (2015, 2018), Jerkstrand et al. (2015), Barbarino et al. (2015), Takáts et al. (2015), Valenti et al. (2015, 2016), Yuan et al. (2016), Dhungana et al. (2016), Terreran et al. (2016), Gutiérrez et al. (2017), Müller et al. (2017), Lisakov et al. (2017), Tomasella et al. (2018), Dastidar et al. (2018), Anderson et al. (2018), Hosseinzadeh et al. (2018), Tartaglia et al. (2018), Tsvetkov et al. (2018).

SE-SNe: Shigeyama et al. (1994), Iwamoto et al. (1994, 1998), Clocchiatti et al. (2000),Nakamura et al. (2001), Stritzinger et al. (2002, 2009), Foley et al. (2003), Mazzali et al. (2003, 2004), Anupama et al. (2005), Deng et al. (2005), Mazzali et al. (2006), Richardson et al. (2006), Tomita et al. (2006), Taubenberger et al. (2006), Folatelli et al. (2006, 2014), Sauer et al. (2006), Tominaga et al. (2008), Valenti et al. (2008, 2011, 2012), Mazzali et al. (2008, 2009, 2017), Silverman et al. (2009), Sahu et al. (2009, 2018), Hamuy et al. (2009), Roming et al. (2009), Drout et al. (2011), Elmhamdi et al. (2011), Taubenberger et al. (2011), Benetti et al. (2011), Ben-Ami et al. (2012), Pignata et al. (2011), Berger et al. (2011), Corsi et al. (2011, 2017), Oates et al. (2012), Bersten et al. (2012, 2018), Sanders et al. (2012a), Bufano et al. (2012, 2014), Melandri et al. (2012, 2014), Milisavljevic et al. (2013a,b, 2015), Takaki et al. (2013), Kumar et al. (2013, 2018), Roy et al. (2013, 2016), Srivastav et al. (2014), Walker et al. (2014), Chen et al. (2014), Morales-Garoffolo et al. (2015), Taddia et al. (2015, 2018), D'Elia et al. (2015), Liu et al. (2015), Prentice et al. (2016), Szalai et al. (2016), Fremling et al. (2016), Lyman et al. (2016), Pian et al. (2017), Cano et al. (2017), Gangopadhyay et al. (2018), Zhang et al. (2018)[11].

[11] From Prentice et al. (2016) the "fully bolometric" values are used.